Intrazeolite Photochemistry. 20. Characterization of Highly Luminescent Europium Complexes inside Zeolites

Mercedes Alvaro,[†] Vicente Fornés,[†] Sara García,[†] Hermenegildo García,*[,†] and J. C. Scaiano*[,‡]

Instituto de Tecnología Química and Departamento de Química, Universidad Politécnica de Valencia, Apartado 22012, 46071 Valencia, Spain, and Department of Chemistry, University of Ottawa, Ottawa K1N 6N5, Canada

Received: January 6, 1998; In Final Form: August 12, 1998

Four organometallic complexes of Eu^{3+} with 2,2′-bipyridine (bipy), benzoyltrifluoroacetone (btfa), 1,10-phenanthroline (phen), and dipicolinic acid (dpic) have been prepared in Y, mordenite, and ZSM-5 zeolites by adsorbing the ligand into Eu^{3+}-doped zeolites. Different samples were obtained varying the Eu^{3+} content and the Eu^{3+}:ligand ratio. Formation of the complexes and their stoichiometry have been assessed by elemental chemical analysis (combustion and atomic absorption) and thermogravimetry-differential scanning calorimetry as well as IR and diffuse reflectance (DR) spectroscopies. The distinctive feature of DR spectra of the solids is the presence of a band of medium intensity in the 500 nm region that is absent for the same complexes in solution. All the samples, including those that do not contain any organic ligand, exhibit room-temperature emission upon laser excitation, although luminescence intensity notably increases upon complexation. The emission lifetimes are in the millisecond time scale and do not follow simple first-order kinetics. Concerning the emission decay, the following observations were made: (i) the complex luminescence is much longer lived inside the zeolites than in solution; (ii) the emission lifetime follows the order dpic > phen > bipy > bfta; (iii) lifetime increases with the amount of the ligand incorporated; (iv) the decays are more rapid as the Eu^{3+} content of the zeolite increases; and (v) emission becomes longer lived in the order ZSM-5 > mordenite > Y. These facts have been rationalized as the result of an increase in the conformational rigidity experienced by the complex that impedes alternative nonemissive deactivation pathways in zeolite media. Dehydration of the solids and subsequent D_2O rehydration does not alter the decay of the uncomplexed Eu^{3+}−Y samples but increases the lifetime of the Eu−btfa complex inside Y zeolite by a factor of 2. This is indicative that emitting Eu^{3+} are not solvated (probably located inside the sodalite cages and hexagonal prisms), while the Eu−btfa complex is coordinated with a single H_2O molecule.

Introduction

Recent progress has been made in the design of highly luminescent europium complexes that can be used as active components for sensors and screens in electronic devices. In this type of metallic complexes light is absorbed by the ligands and, then, the energy transferred to the emitting metal ion (*antenna effect*).[1−6] To study the photophysical properties in solution, Eu^{3+} complexes have been synthesized from soluble salts of this lanthanide ion adding ligands such as 2,2′-bipyridine (bipy),[7,8] benzoyltrifluoroacetone[9] (btfa), 1,10-phenanthroline (phen),[10] and dipicolinic acid (dpic)[11−14] Aqueous solutions of Eu^{3+} do not fluoresce owing to the efficient radiationless deactivation mechanism occurring in the *aqua* complex involving energy transfer from excited Eu^{3+} to the vibrational levels of the OH groups which decay rapidly in a nonemissive way.[15−17] In contrast, many organometallic complexes of Eu^{3+} are luminescent in aqueous medium because the organic ligands displace the H_2O molecules, shielding the Eu^{3+} and enhancing the emission quantum yield.[18] Furthermore, aromatic ligands have a characteristic UV/vis absorption spectrum at longer wavelengths than that of the *aqua* Eu^{3+} complex, thus expanding the range of excitation energies.[19] The structures of these complexes have been confirmed in some cases by X-ray diffraction.[10,20,21] They display a long emission lifetime in the millisecond time scale and high quantum yields even at room temperature.[22]

Zeolites have been found to be suitable media to control the photophysical properties of the embedded organic guest molecules.[23−26] Herein we have prepared a series of four europium complexes incorporated into three different zeolites, in which we have varied the Eu^{3+} content, the nature of the ligand, and the zeolite crystalline structure. Our aim has been to establish to what extent these parameters influence the luminescent properties of the Eu^{3+} complexes encapsulated within the confined spaces of zeolites. Related to our work are the reports on the photophysical and photochemical properties of $Ru(bipy)_3^{2+}$ and $Mn(bipy)_2^{2+}$ inside Y zeolite.[27−31] Chemiluminescence of europium exchanged Y zeolite upon thermal decomposition of tetramethyl-1,2-dioxetane has also been reported.[32]

Zeolites are microporous crystalline aluminosilicates, whose general formula corresponds to $M^{n+}_{x/n}[(AlO_2)_x(SiO_2)_y]mH_2O$.[33−35] Their structure is formed by a three-directional network of $[AlO_4]^{5-}$ and $[SiO_4]^{4-}$ tetrahedra linked via bridging oxygen atoms. When a silicon is isomorphically replaced by one aluminum atom, one negative charge is generated in the framework. To compensate this negative charge, associated cations (M^{n+}) must be present into the micropores. These

[†] Universidad Politecnica de Valencia.
[‡] University of Ottawa.

10.1021/jp980669g CCC: $15.00
Published on Web 10/08/1998

TABLE 1: Nomenclature and Analytical Data of the Eu^{3+}-Doped Zeolites Studied in This Work

entry	parent zeolite	sample containing Eu^{3+} complex	content (mmol × g^{-1}) Eu^{3+}	content (mmol × g^{-1}) ligand[a]
1	Eu−Y-1		0.41	0.00
2		Eu-bipy-Y-1		0.41
3		Eu-btfa-Y-1a		0.04
4		Eu-btfa-Y-1b		0.46
5		Eu-dpic-Y-1		0.55
6		Eu-phen-Y-1		0.74
7	Eu−Y-2		0.58	0.00
8		Eu-bipy-Y-2		0.48
9		Eu-btfa-Y-2a		0.06
10		Eu-btfa-Y-2b		0.38
11		Eu-dpic-Y-2a		0.07
12		Eu-dpic-Y-2b		0.30
13		Eu-phen-Y-2		0.74
14	Eu−Y-3		0.71	0.00
15		Eu-bipy-Y-3a		0.38
16		Eu-bipy-Y-3b		1.73
17		Eu-btfa-Y-3a		0.42
18		Eu-btfa-Y-3b		0.96
19		Eu-dpic-Y-3a		0.80
20		Eu-dpic-Y-3b		1.52
21		Eu-phen-Y-3a		1.10
22		Eu-phen-Y-3b		1.46
23	Eu−Y-4		0.89	0.00
24	Eu−Mor		0.38	0.00
25		Eu-bipy-Mor-a		0.14
26		Eu-bipy-Mor-b		0.59
27		Eu-bipy-Mor-c		0.85
28		Eu-btfa-Mor-a		0.19
29		Eu-btfa-Mor-b		0.21
30		Eu-dpic-Mor		0.28
31		Eu-phen-Mor		0.83
32	Eu−ZSM-5		0.02	0.00
33		Eu-bipy-ZSM-5		0.42

[a] Measured by combustion chemical (C and N) analysis.

cations are ionically bound to the zeolite framework and can be readily exchanged by other cations such as Eu^{3+} and rare earth ions. The framework structures create uniform cages or channels of strictly regular dimensions, which are normally filled with water. When dehydrated, other guest molecules can occupy the voids as long as the internal spaces are large enough to accommodate the guest, and the aperture sizes allow passage of the substrates. In zeolites it is possible to vary the chemical composition as well as to choose among the available framework structures. The free volume of the pores varies depending on the zeolite and this may determine the stoichiometry of the complex (confinement) as well as on the number of Eu^{3+} ions and their proximity.

Results and Discussion

I. Characterization of the Complexes inside Zeolites. Eu^{3+} was introduced starting from the Na^+-form of the corresponding zeolite by ion exchange using aqueous solutions of $Eu(NO_3)_3$ at pH 3.[36] Eu^{3+} content of the zeolites was, then, determined by quantitative atomic absorption spectroscopy after disggregation of the solid. Alternatively, the amount of Eu^{3+} introduced in the zeolite by ion exchange can also be determined by diffuse reflectance spectroscopy (DRS). Thus, the original Na^+-form of our zeolites do not have any defined absorption band above 200 nm. In contrast, Eu^{3+}-doping gives rise to the appearance of a new band at 240 nm attributable to the presence of $Eu(H_2O)_n^{3+}$ *aqua* complex inside the zeolites. The intensity of this 240 nm band allows for quantification of the Eu^{3+} content in a more simple and convenient way than atomic absorption

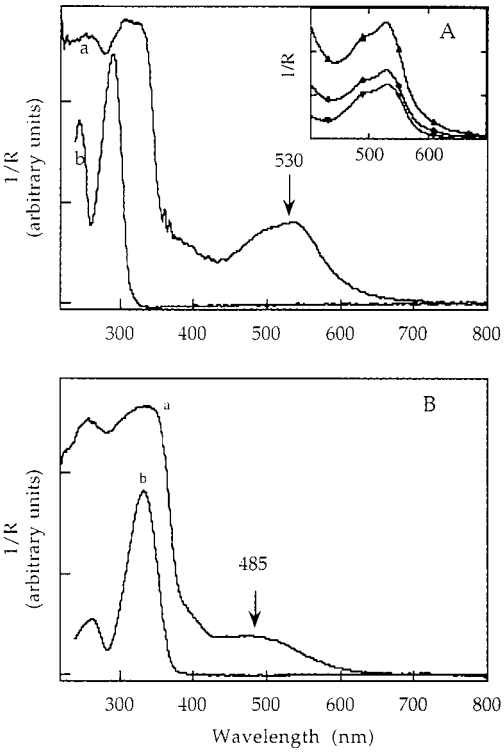

Figure 1. (A) DR spectra (plotted as the inverse of the reflectivity, $1/R$) of Eu-bipy-Y-3b (curve a) and UV−vis absorption spectrum of a solution of bipy in CH_2Cl_2 (curve b). The insert shows the detail of the 530 nm band of the Eu-bipy-Y-3b before and after impregnation with NaBr (◆) and NaI. (B) DR spectrum of Eu-btfa-Y-1b (a) compared to that of an authentic sample of $Eu(btfa)_3$ in ethanol (b). The arrow indicates the wavelength of the band.

CHART 1

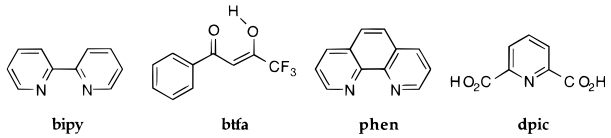

spectroscopy. Zeolite Y was prepared at four different levels of ion exchange (Table 1). Not surprisingly, the ion exchange percentage achieved in ZSM-5 was the lowest among the three zeolites owing to the impeded diffusion of the relatively bulky Eu^{3+} *aqua* complex through the medium pore channels (5.4 × 5.6 Å^2) of the pentasil zeolite. In fact, the effective kinetic diameter of hydrated Eu^{3+} not only involves nine water molecules of its first coordination sphere but also a dynamic double solvation layer.[37−39]

The complexes were prepared by allowing free diffusion of the ligands (see Chart 1) from an organic solution to the Eu^{3+}-doped zeolites. The choice of these ligands is based on the reported luminescence of the corresponding complexes in solution.[14,20,40] The amount of ligand adsorbed in each sample was established by combustion chemical analysis (C and N) as well as by thermogravimetry. The nomenclature of the samples studied, their unit cell composition and ligand loading are summarized in Table 1.

Formation of the Eu^{3+} complexes can be conveniently followed by DRS (Figure 1). Thus, all Eu^{3+} complexes inside zeolites exhibited in the UV−vis spectrum as the most characteristic absorption a broad band of medium intensity at about 500 nm. Another intense absorption around 320 nm in the UV is common for the Eu^{3+} complex in solution and in zeolites, although in the latter case it is remarkably broader.

The ligands also possess a UV band in the same region although significantly blue-shifted with respect to the complex. The same effect has been previously observed for related Eu^{3+} complexes in solution.[40]

The visible band around 500 nm is only clearly observable for the DR spectra of the Eu^{3+} complexes included in zeolites but not for the corresponding complexes in solution. In the case of dipicolinate complexes in aqueous solutions, this absorption at 530 nm has been found to be very weak and hardly detectable.[41] For $Eu(dpic)_3^{3-}$ complex in H_2O, this band has been attributed[41] to a *hypersensitive transition*, so-called because their intensity depends largely on the environment of the lanthanide ion.[42]

We wanted to give some support to the hypersensitive nature of the visible band appearing for the Eu^{3+} complexes encapsulated within zeolites. Aimed at this purpose, the Eu-bipy-Y-3b was impregnated with NaBr and NaI. It is known that for the same type of complex the intensity of a hypersensitive transition increases in the series $H_2O < Br^- < I^-$.[41] The results obtained (see insert of Figure 1A) showed the expected trend for this type of transitions.

The reason the intensity of these hypersensitive transitions increases so remarkably upon incorporation within the zeolite pores may be related to distortions in the symmetry of the guest when it is confined in a restricted space whose dimensions are close to its molecular size.[43−46] These modifications with respect to the solution complex would produce variations in the allowness and efficiency of a particular electronic transition. In this context, it has been reported that the optical spectrum of β-carotene inside the channels of ZSM-5 exhibits a new band corresponding to the transition between the 0,0 vibrational levels of $^0S \rightarrow {}^1S$ that is forbidden and not observed in solution.[47] We have also reported a general increase in the extinction coefficients of the visible bands when a chromophore is incorporated inside medium and large pore zeolites.[23,48] A related precedent on the appearance of a new band in the visible for $Mn(bipy)_2^{2+}$ in faujasite and EMT zeolites not observed for the same complex in solution can be found in the literature.[31]

A definite piece of evidence proving that the complexes have been successfully formed was obtained by IR spectroscopy. In the case of btfa, this ligand exhibits a C═O vibration band at 1670 cm^{-1} that disappears after complexation of its enolate form (eq 1).

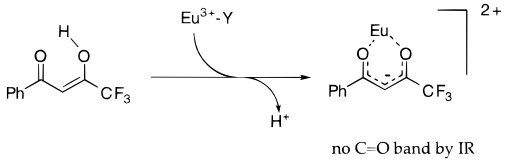

(1)

Notably, the IR spectrum recorded for the Eu^{3+}-doped Y zeolite after incorporation of btfa coincides remarkably well with that obtained for the same complex prepared in solution according to reported procedures, being different from that corresponding to uncomplexed btfa ligand (Figure 2).[11] The good match between IR spectra constitutes firm evidence supporting the identity and purity of the Eu^{3+} complexes prepared inside the zeolite.

The situation of the Eu−btfa complex inside mordenite deserves comment. The stoichiometry of this complex in solution has been determined[11] as $Eu(btfa)_3(H_2O)_2$. The size of this complex appears to be too large to be accommodated inside the channels of mordenite (≈7 Å).[49] Molecular modeling at semiempirical level clearly establishes that there is certainly

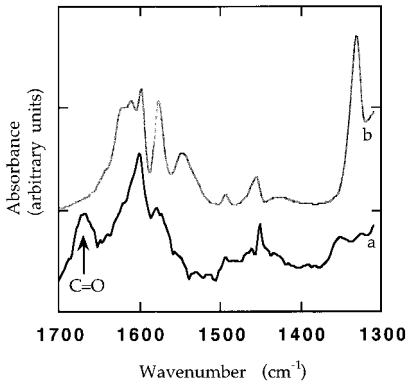

Figure 2. IR spectra of btfa ligand recorded on inert silicon plate (curve a) and that of the Eu-btfa-Y-3b sample (curve b). In the latter case, to eliminate interference of H_2O the zeolite was outgassed at 100 °C under 10^{-2} Pa for 1 h before recording the spectrum at room temperature. The absorption of btfa attributable to the C═O stretching band has been indicated with an arrow.

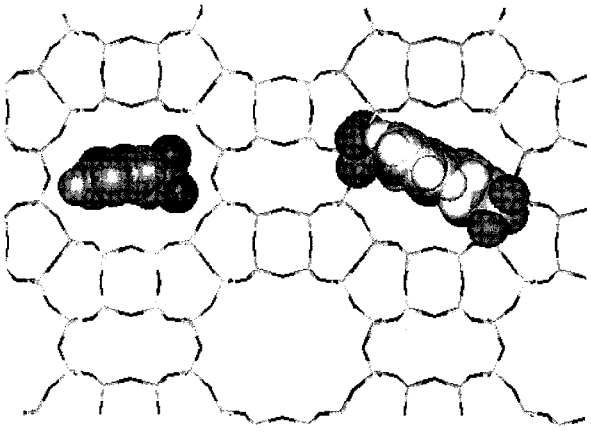

Figure 3. Molecular modeling of optimized (semiempirical level) geometry of btfa (left) and square planar $Eu(btfa)_2^+$ (right) docked inside the channels of mordenite.

not enough space inside the mordenite channels to include $Eu(btfa)_3$ or even a planar $Eu(btfa)_2^+$ complex (Figure 3). However, both DR and IR spectra of Eu−btfa complex in zeolite Y (where much less space restrictions are expected) are indistinguishable of the spectra of Eu-btfa-Mor-b.

Taking into account that IR spectroscopy reports mainly on the structure of the ligand, the observed IR spectrum of Eu-btfa-Mor-b corresponds to complexed enolate anion and not to neutral btfa (eq 1). An explanation that would reconcile all these facts would be to assume a $Eu(bfta)^{2+}$ stoichiometry for the complex inside mordenite. The negative oxygens of the lattice and/or coadsorbed water would complete the coordination sphere of Eu^{3+} ions inside the zeolite. In this sense, perusal of Table 1 reveals that in general most of our samples have a Eu: ligand ratio much higher than the minimum achievable in solution. In particular for the case of Eu−btfa the minimum metal-to-ligand ratio measured was 1:1.35 for Y zeolite (entry 18), and there are some examples in which all or most of the Eu^{3+} ions are not bound to btfa (see entries 3 and 9).

Since complexation is a stepwise equilibrium (eq 2), our assumption is that depending on the bfta content and the available space surrounding Eu^{3+} only the first equilibrium may be established, while the second and third can be completely unfavorable inside zeolites due to steric restrictions. A recent study about the influence of the Eu:dipicolinate ratio has reported that the most abundant species of the Eu(III) in aqueous solutions is $Eu(dpic)^+$ when the ratio is 1:1.[41]

$$Eu^{3+} + bfta \rightleftharpoons Eu(bfta)^{2+} + H^+ \quad K1$$

$$Eu(bfta)^{2+} + bfta \rightleftharpoons Eu(bbfta)_2^{+} + H^+ \quad K2 \qquad (2)$$

$$Eu(bfta)_2^{+} + bfta \rightleftharpoons Eu(bfta)_3 + H^+ \quad K3$$

On the other hand, IR spectroscopy also gives interesting information on the fate of the ligand in the Eu−bipy complex included in the zeolite. Pyridine is widely used as probe molecule for the characterization of Brönsted and Lewis sites in acid zeolites.[50,51] It has been firmly established that specific aromatic stretching bands can be used to determine the presence of pyH^+ (pyridinium ions) or pyridine−Lewis adducts. Thus, the band at 1550 cm^{-1} corresponds to pyH^+ (Brönsted sites), while the band at 1450 cm^{-1} indicates the presence of Lewis sites. In the context of acidity measurements, detailed studies of the pyridine adsorption in rare earth-exchanged zeolites are available in the literature.[52]

Bipy has a chemical structure closely related to pyridine. We have observed in the IR spectrum of Eu-bipy-Y-2 sample these two bands attributable to protonated bipy-H^+ ion and to bipy acting as ligand complexing Eu^{3+} ion (Lewis adduct) (Figure 4).

Thus, the presence of the 1434 cm^{-1} band is in agreement with the formation of the Eu−bipy complex, being consistent with the corresponding DRS (see Figure 1). On the other hand, the appearance of an additional band at 1530 cm^{-1} in the IR spectrum of Eu-bipy-Y-2 also indicates the presence of some $bipyH^+$ arising by protonation of basic bipy. With regard to the formation of bipy-H^+, the generation of Brönsted sites in rare earth-exchanged zeolites is well documented in the literature[53−55] and has found application in the use of rare earth-exchanged zeolites as acid catalyts.[56,57] In our case, the IR spectrum of calcined Eu-Y-1 (without any ligand) gives an intense O−H stretching band at 3500 cm^{-1} that corresponds to $Eu(OH)^{2+}$ species indicative of the presence of concomitant H^+. According to eq 3, $Eu(OH)^{2+}$ arises from the thermolysis of hydrated Eu^{3+} during calcination of the zeolite at high temperatures.

$$Eu(H_2O)_x^{3+} \rightarrow Eu(H_2O)_{x-1}(OH)^{2+} + H^+$$

$$bipy + H^+ \rightleftharpoons bipy\text{-}H^+ \qquad (3)$$

These adventitious H^+ would protonate a fraction of bipy during the incorporation of this basic molecule, giving rise to the observed pyridinium band in the IR. However, it should be noted that despite the presence of some bipy-H^+, the band at 1434 cm^{-1} can be safely assigned to Eu coordinated to bipy, thus, proving that Eu−bipy complex is present inside the zeolite.

II. Luminescence Measurements. All the samples indicated in Table 1, including those that do not contain organic ligand, exhibit room-temperature emission upon laser excitation at 266 nm. The luminescence spectra were recorded using a CCD camera and were essentially identical within the resolution limit of the technique. They consist of two broad emissions, a weak one at 595 and a second more intense band at 615 nm, lacking fine structure. These spectra are characteristic of the $^5D_0 \rightarrow {}^7J$ transition of the lanthanide ion. A representative example is shown in Figure 5.

Decay profiles were measured at the wavelength of the maximum of the spectra using a photomultiplier/oscilloscope system. As anticipated, they were in all cases in the millisecond time scale. The emission decays could not be fitted either to simple first-order kinetics or to two overimposed first-order decays. For instance, by applying first-order kinetics the data corresponding to the $Eu(phen)^{3+}$ complex in mordenite gives an emission lifetime $\tau = 0.652$ ms (Chisq = 4269.8, $R = 0.99445$). The curve fit only improved slightly (Chisq = 3106.4, $R = 0.99600$) by analyzing this decay as a series of two first-order decays giving a predominant faster component ($\tau_1 = 0.372$ ms, 55%) and a slower second decay ($\tau_2 = 1.469$ ms, 45%). This is commonly interpreted as a reflection of the inhomogeneity of the emiting species in terms of different type of complexes as well as their different location with respect to the host media. Since the purpose of this work is a direct comparison of the decays in different zeolites, a detailed kinetic analysis was not pursued.

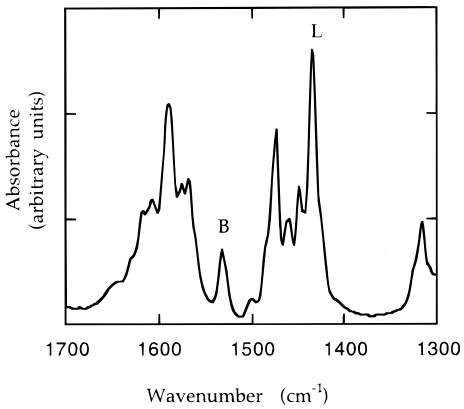

Figure 4. Aromatic region of the IR spectrum of Eu-bipy-Y-3b showing the bands that can be attributed as specific of protonated (B) and complexed (L) bipy.

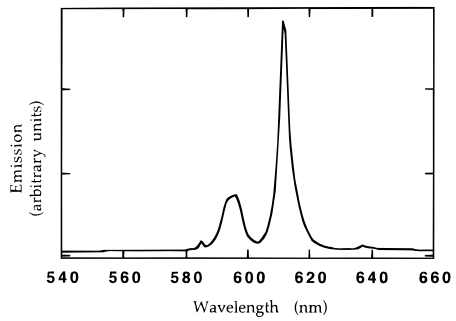

Figure 5. Luminescence of Eu^{3+} recorded at room temperature for the sample Eu-dpic-Y-1 under ambient atmosphere.

The intensity of the emission from the solid samples increases dramatically after adsorption of the ligands, thus, following the same pattern observed in solution. According to the previous spectroscopic characterization of our zeolites, it can be assumed that the organic ligands strongly bind Eu^{3+} ions resident within the zeolite internal voids, partly removing H_2O and/or OH^- oscillators from its first coordination sphere. This shielding of the lanthanide ion from OH groups would result in an enhancement of the emissive mechanism of the Eu^{3+} excited state.

More remarkable is, however, the luminescence observed for those zeolites that do not contain organic ligand. Given that coadsorbed water is present inside the zeolites (see Experimental Section for the water content), this emission from hydrated Eu^{3+}-doped zeolites contrasts with the lack of measurable luminescence observed for the *aqua*−Eu^{3+} complexes in solution. Analogous emission from uncomplexed Eu^{3+} hosted in titanate layered oxides has also been recently reported.[58]

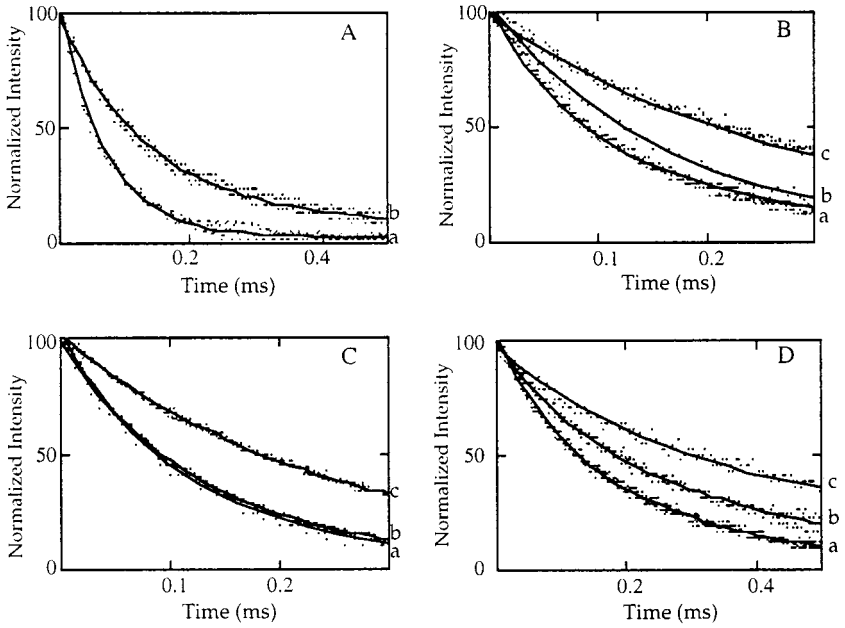

Figure 6. (A) Luminescence decay at 590 nm measured at room temperature under ambient atmosphere of an ethanolic solution of $Eu(btfa)_3$ (curve a) and of the sample Eu-btfa-Y-3a (curve b). The continuous lines correspond to the best fit of the experimental points. (B) Same as (A) for three zeolites increasing the Eu^{3+} content: Eu-btfa-Y-3b (curve a), Eu-btfa-Y-2b (curve b), and Eu-bfta-Y-1b (curve c). (C) Same as (A) for three zeolites varying the amount of ligand: Eu-Y-2 (a), Eu-btfa-Y-2a (b), and Eu-btfa-Y-2b (c). (D) Same as (A) for three samples varying the zeolite crystal structure: Eu-bipy-Y-1 (a), Eu-bipy-Mor-b (b), and Eu-bipy-ZSM-5 (c).

A possible rationalization for this fact is based on the different locations of the charge-balancing cations in the zeolite micropores. Thus, for faujasites it is known that cations can occupy three sites (Scheme 1). Only one of them, type SIII corresponding to cations located inside the large supercage, have enough space to be fully hydrated as in the *nonaaqua* complex in solution. Sites I and II, located inside the small sodalite cage and the hexagonal prism, have the cation tightly *solvated* by the lattice oxygens (similar to a crown ether) and cannot be hydrated. In detailed studies of the location of rare earth-exchanged faujasites, it has been reported that the lanthanide ions are initially introduced at the more accessible SIII type, but during calcination at high temperatures a considerable fraction of these lanthanides migrates to SI and SII sites.[53−55] We speculate that the emission observed for Eu^{3+}-doped zeolites containing no organic ligand would be due specifically to these SI and SII populations.

SCHEME 1

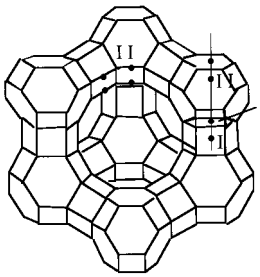

To seek some evidence for this assumption, the Eu-Y-3 sample was dehydrated and rehydrated either with H_2O or D_2O. It is well-known that the emission lifetime of Eu^{3+} complexes in aqueous solutions increases along the molar fraction of D_2O, being the longest lived in pure D_2O.[37] No difference in the luminescence decay profiles between the Eu-Y-3 samples treated with H_2O or D_2O (loading of nine water molecules per supercage determined by thermogravimetry) was observed, thus, supporting our hypothesis that luminescent Eu^{3+} correspond to the fraction of unsolvated ions at sites SI and SII (Scheme 1).

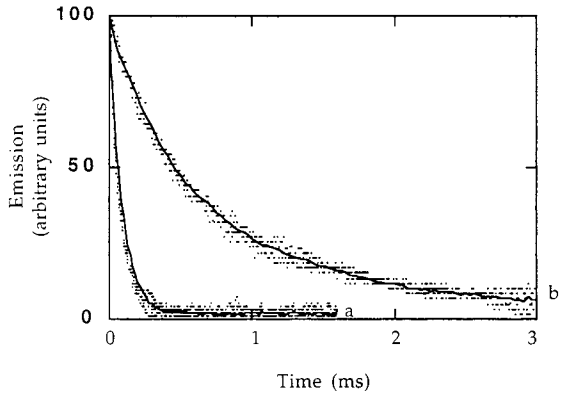

Figure 7. Comparison between the emission decay of the $Eu(btfa)_3$ complex in ethanolic solution (plot a) and that of the solid Eu-phen-Mor (plot b).

Comparison of the emission decays of the different samples leads to the following observations:

(i) The complexes are longer lived inside zeolites than in solution.

(ii) The nature of the ligand influences the decay of the luminescence; the order of the emission lifetime is dpic > phen > bipy > bfta.

(iii) The lifetime of the emission increases with the amount of the ligand incorporated in the zeolite. Eu^{3+}-doped zeolites with no ligand are much shorter lived.

(iv)The luminescence decays more rapidly as the Eu^{3+} content of the zeolite increases.

(v) The zeolite crystal structure influences the decay profile. The emission becomes longer lived in the order ZSM-5 > mordenite > Y.

Some selected examples to support the above points are presented in Figure 6, while Figure 7 provides a comparison of the luminescence decay in solution and inside mordenite.

Most of the above observations can be rationalized on the basis of the formation the Eu^{3+} complexes inside the zeolite, assuming that inmobilization of the complex increases its lifetime by inhibiting nonradiative deactivation pathways usually associated to fast motions in the emiting species. Remarkable examples of nonemiting species in solution that fluoresce in zeolites have been previously reported by us.[23,25,59] Thus, depending on the incorporated ligand some changes in the lifetime should be expected (point ii). Their lifetime will increase upon incorporation in a confined space (point i) and along the dimension of this cavity is reduced (point v). In addition, it appears also that self-quenching by uncomplexed Eu^{3+} can be operating in some extent. This would explain why lower Eu^{3+} or higher ligand content (points iii and iv) lead to an increase in the lifetime of the emission.

Finally, a point of interest was to determine whether the emission lifetime of the zeolite encapsulated complexes is influenced by the presence of solvating H_2O molecules. To address this point the Eu-btfa-Y-3b sample was dehydrated and rehydrated with H_2O or D_2O. While submitting of the Eu-btfa-Y-3b sample to the evacuation/rehydration cycle with H_2O does not influence its emission decay, the sample treated with D_2O (an average of 4.7 molecules per supercage determined by thermogravimetry) increases the emission lifetime approximately by a factor of 2 (estimated from the best fit to a monoexponential decay, vide supra for the comment on the curve fitting). According to eq 4 that correlates the variation in the luminescence lifetimes and the number of coordinated water molecules,[37] the encapsulated Eu-btfa-Y-3b complex is coordinated with a single H_2O molecule. It is worth noting that we could not observe luminescence with the CCD camera from a H_2O solution of unsupported Eu-btfa, while the lifetime of Eu-btfa in D_2O is 0.27 ms.

$$n^\circ = A_{Eu} \times (\tau^{-1}_{H_2O} - \tau^{-1}_{D_2O}) \quad (4)$$

Conclusions

Incorporation of a guest in organized and heterogeneous media is a general methodology that allows a certain control in the deactivation pathways of the excited states. Herein we have shown that conformation rigidity plays an important role in the deactivation of the excited state of europium. Thus, by forming the europium complexes inside a series of zeolites with a progressive reduction of the space surrounding the complex, longer lived emission is observed. This effect also occurs even in those cases in which the highest ligand:metal stoichiometry for the complex cannot be achieved despite the presence of large amount of coadsorbed H_2O. In this way, we have produced samples in which the emission is more than 10-fold longer lived than that recorded for the same type of complex in solution.

Experimental Section

Samples of zeolites Eu-Y-1 ($Eu_6Na_{35}Al_{53}Si_{139}O_{384}\cdot 223H_2O$, 0.75 Eu^{3+} per supercage), Eu-Mor ($Eu_{1.2}Na_{2.9}Al_{6.5}Si_{41.5}O_{384}\cdot H_2O$, 55% of the total ion exchange capacity), and Eu-ZSM-5 ($Eu_{0.13}Na_{4.2}Al_{4.6}Si_{92}O_{193.2}\cdot 14H_2O$, 8.5% of the total ion exchange capacity) were obtained starting from NaY (P. Q., Si/Al 2.6), NaMor (P. Q., mordenite, Si/Al 10), and NaZSM-5 (synthesized according to the patent literature,[60] Si/Al 17.5) by ion exchange using aqueous solutions (pH 3) of $Eu(NO_3)_3$ (0.05 M) in a solid:liquid ratio 1:10 wt %. Three other solutions of $Eu(NO_3)_3$ of increasing concentrations (0.1, 0.20, and 0.25 M, respectively) were also used to increase the percentage of ion exchange to produce the samples Eu-Y-2 ($Eu_{8.5}Na_{27.5}Al_{53}Si_{139}O_{384}\cdot 86H_2O$, 1.06 Eu^{3+} per supercage), Eu-Y-3 ($Eu_{11}Na_{20}Al_{53}Si_{139}O_{384}\cdot 74H_2O$, 1.4 Eu^{3+} per supercage), and Eu-Y-4 ($Eu_{13}Na_{14}Al_{53}Si_{139}O_{384}\cdot 74H_2O$, 1.6 Eu^{3+} per supercage). After Eu^{3+}-Na^+ ion exchange, the corresponding ligand (phen, bipy, btfa and dpa, Aldrich used as received) was absorbed by stirring for 24 h a suspension of thermally dehydrated (overnight, 200 °C) zeolite (300 mg) in 3 mL of a solution in ethanol of the ligand at different concentrations. Subsequently the samples were filtered, washed with fresh ethanol, and stored in a dissecator (anhydrous CaO) until their use. $Eu(btfa)_2(H_2O)_2$ complex was obtained by recrystallization in ethanol of a solution of Eu^{3+} (from Eu_2O_3) and btfa following reported procedures.[11] Impregnation with NaBr and NaI was accomplished by stirring magnetically for 2 h at room temperature a suspension of Eu-bipy-Y-3b (200 mg) with a 0.5 M aqueous solution of NaBr or NaI using a liquid:solid weight ratio of 10.

For the experiments with coadsorbed D_2O, the corresponding Eu-Y-3 or Eu-btfa-Y-3b samples (200 mg) were heated in an oven at 150 °C for 5 h. After this time, the solid was cooled below 100 °C and poured into H_2O or D_2O (98%) (2 mL), and the suspension was stirred for 20 min. After filtration, the solid was dried and used before it has elapsed 2 h of the dehydration/rehydration cycle.

The percentage of Eu^{3+} exchange was quantitatively determined by atomic absorption spectroscopy of the Eu^{3+} as well as the remaining Na^+ after disggregation of the solids with concentrated HF at 60 °C. The H_2O or D_2O coadsorbed on the zeolites was obtained by thermogravimetry (Netzsch STA 409 thermobalance), measuring the loss of weight upon heating the samples from room temperature up to 200 °C. The amount of ligand adsorbed was determined by combustion chemical analyses of C and N (when appropriate) using a Perkin-Elmer analyzer. DR spectra were obtained in a Shimadzu UV-2021 PC spectrophotometer having an integrating sphere accessory. FT-IR spectra of complexes in zeolites were recorded at room temperature using a greaseless CaF_2 cell in a Nicolet 710 FT spectrophotometer. Self-supported wafers (~10 mg) were prepared by compressing the zeolite powder at 1 Ton × cm^2. The samples were outgassed at 100 °C under 10^{-2} Pa for 1 h before recording the IR spectra.

Luminescence spectra were recorded in an Oriel Intaspec V CCD camera upon excitation with the fourth harmonic of the output of a Spectron Nd:YAG laser (266 nm, ≤ 10 ns fwhp, ≤ 10 mJ × $pulse^{-1}$). Decay profiles were measured with a Oriel 77341 photomultiplier coupled to a Tektronix TDS 640 A oscilloscope. Emission light from the samples was collected through a fiber optic system. Zeolites were placed in an open powder cell, the laser beam hiting directly the solid surface. For luminescence spectra in solution, 7 × 7 mm^2 Suprasil quartz cuvettes were used.

References and Notes

(1) Sabbatini, N.; Mecati, A.; Guardigli, M.; Balzani, V.; Lehn, J.-M.; Zeissel, R.; Ungaro, R. *J. Luminesc.* **1991**, *48/49*, 463.

(2) Sabbatini, N.; Guardigl, M.; Lehn, J.-M. *Coord. Chem. Rev.* **1993**, *123*, 201.

(3) Balzani, V.; Scandola, F. *Supramolecular Photochemistry*; Horwood, England: Chichester, 1991.

(4) Balzani, V. *Tetrahedron* **1992**, *48*, 10443−10514.

(5) Galaup, C.; Picard, C.; Cazaux, L.; Tisnés, P.; Aspe, D.; Autiero, H. *New J. Chem.* **1996**, *20*, 997−999.

(6) Bodar-Houillon, F.; Marsura, A. *New J. Chem.* **1996**, *20*, 1041−1045.

(7) Ulrich, G.; Hissler, M.; Ziessel, R.; Manet, I.; Sarti, G.; Sabbatini, N. *New J. Chem.* **1997**, *21*, 147−150.

(8) Armaroli, N.; Balzani, V.; Barigelletti, F.; Ward, M. D.; McCleverti, J. A. *Chem. Phys. Lett.* **1997**, *276*, 435−440.

(9) de Sá, G. F.; de Silva, F. R. G.; Malta, O. L. *J. Alloys Compd.* **1994**, *207/208*, 457.
(10) Lu, W.; Cheng, Y.; Dong, N.; Gu, J.; Xu, C. *Acta Crystallogr.* **1995**, *C51*, 2295−2299.
(11) de Mello Donegá, C.; Junior, S. A.; de Sá, G. F. *J. Chem. Soc., Chem. Commun.* **1996**, 1199−1200.
(12) Barela, T. D.; Sherry, A. D. *Anal. Biochem.* **1976**, *76*, 351−357.
(13) Lamture, J. B.; Wensel, T. G. *Tetrahedron Lett.* **1993**, *34*, 4141−4144.
(14) Lamture, J. B.; Iverson, B.; Hogan, M. E. *Tetrahedron Lett.* **1996**, *37*, 6483−6486.
(15) Kropp, J. L.; Windsor, M. W. *J. Chem. Phys.* **1965**, *42*, 1599.
(16) Haas, Y.; Stein, G. *J. Chem. Phys.* **1972**, *76*, 1093.
(17) Dickins, R. S.; Parker, D.; de Sousa, A. S.; Williams, J. A. G. *J. Chem. Soc., Chem. Commun.* **1996**, 697−698.
(18) Horrocks, W. D., Jr.; Sudnick, D. R. *Acc. Chem. Res.* ***1981***, *14*, 384.
(19) Serra, O. A.; Nassar, E. J.; G., Z.; Rosa, I. L. V. *J. Alloys Compd.* **1994**, *207/208*, 454−456.
(20) Brayshaw, P. A.; Harrowfield, J. M.; Sobolev, A. N. *Acta Crystallogr.* **1995**, *C51*, 1799−1802.
(21) Dossing, A.; Toftlund, H.; Hazell, A.; Bourassa, J.; Ford, P. C. *J. Chem. Soc., Dalton Trans*, **1997**, 335−339.
(22) Soini, E.; Lovgren, T. *CRC Crit. Rev. Anal. Chem.* **1987**, *10*, 105−154.
(23) Cano, M. L.; Cozens, F. L.; Fornés, V.; García, H.; Scaiano, J. C. *J. Phys. Chem.* **1996**, *100*, 18145−18151.
(24) Cano, M. L.; Cozens, F. L.; García, H.; Martí, V.; Scaiano, J. C. *J. Phys. Chem.* **1996**, *100*, 18152−18157.
(25) Alvaro, M.; Facey, G. A.; García, H.; García, S.; Scaiano, J. C. *J. Phys. Chem.* **1996**, *100*, 18173−18176.
(26) García, H.; García, S.; Pérez-Prieto, J.; Scaiano, J. C. *J. Phys. Chem.*, **1996**, *100*, 18158−18164.
(27) Dutta, P. K.; Turbeville, W. *J. Phys. Chem.* **1992**, *96*, 9410−9416.
(28) Dutta, P. K.; Turbeville, W.; Robins, D. S. *J. Phys. Chem.* **1992**, *96*, 5024−5029.
(29) Dutta, P. K.; Ledney, M. *J. Am. Chem. Soc.* **1995**, *117*, 7687−7695.
(30) Dutta, P. K. *J. Incl. Phenom. Mol. Recognition. Chem.* **1995**, *21*, 215−237.
(31) Knops-Gerrits, P.-P. H. J. M.; De Schryver, F. C.; van der Auweraer, M.; van Mingroot, H.; Li, X.-y.; Jacobs, P. A. *Chem. Eur. J.* **1996**, *2*, 592−597.
(32) Benedict, B. L.; Ellis, A. B. *Tetrahedron* **1987**, *43*, 1625−1633.
(33) Barrer, R. M. *Zeolites and Clay Minerals as Sorbents and Molecular Sieves*; Academic Press: London, 1978.
(34) Breck, D. W. *Zeolite Molecular Sieves: Structure, Chemistry and Use*; John Wiley and Sons: New York, 1974.
(35) *Introduction to Zeolite Science and Practice*; van Bekkum, H., Flanigen, E. M., Jansen, J. C., Eds.; Elsevier: Amsterdam, 1991.
(36) Acid pHs avoid hydrolysis of solvated nonaaqua $Eu(H_2O)_9^{3+}$ complex to the corresponding mono hydroxide $Eu(H_2O)_8(OH)^{2+}$ that would make the ion exchange uncertain and less efficient.
(37) Horrocks, W. D.; Sundnick, D. R. *J. Am. Chem. Soc.* **1979**, *101*, 334.
(38) Takahashi, Y.; Kimura, T.; Kato, Y.; Minai, Y.; Tominaga, T. *J. Chem. Soc., Chem. Commun.* **1997**, 223−224.
(39) David, F. H.; Fourest, B. *New J. Chem.* **1997**, *21*, 167−176.
(40) Prodi, L.; Maestri, M.; Ziessel, R.; Balzani, V. *Inorg. Chem.* **1991**, *30*, 3798−3802.
(41) Peacock, R. D. *Structure Bonding* **1975**, *22*, 83.
(42) Binnemans, K.; van Herck, K.; Görller-Walrand, C. *Chem. Phys. Lett.* **1997**, *266*, 297−302.
(43) Zicovich-Wilson, C.; Planelles, J. H.; Jaskólski, W. *Int. J. Quantum Chem.* **1994**, *50*, 429−444.
(44) Zicovich-Wilson, C. M.; Corma, A.; Viruela, P. *J. Phys. Chem.* **1994**, *98*, 10863−10870.
(45) Corma, A.; Zicovich-Wilson, C.; Viruela, P. *J. Phys. Chem.* **1994**, *98*, 10863−10870.
(46) Corma, A.; García, H.; Sastre, G.; Viruela, P. M. *J. Phys. Chem. B* **1997**, *101*, 4575−4582.
(47) Haley, J. L.; Fitch, A. N.; Goyal, R.; Lambert, C.; Truscott, T. G.; Chacon, J. N.; Stirling, D.; Schalch, W. *J. Chem. Soc., Chem. Commun.* **1992**, 1175−1176.
(48) Baldoví, M. V.; Cozens, F. L.; Fornés, V.; García, H.; Scaiano, J. C. *Chem. Mater.* **1996**, *8*, 152−160.
(49) Meier, W. M.; Olson, D. H.; Baerlocher, C. *Zeolites* **1996**, *17*, 1−229.
(50) Arribas, J.; Corma, A.; Fornés, V. *J. Catal.* **1984**, *88*, 374−380.
(51) Corma, A. *Chem. Rev.* **1995**, *95*, 559−614.
(52) Ward, R. J.; Bodner, G. M. *J. Chem. Educ.* **1993**, *70*, 198−199.
(53) Lee, E. F. T.; Rees, L. V. C. *Zeolites* **1987**, *7*, 143−147.
(54) Lee, E. F. T.; Rees, L. V. C. *Zeolites* **1987**, *7*, 545−548.
(55) Keir, D.; Lee, E. F. T.; Rees, L. V. C. *Zeolites* **1988**, *8*, 228−231.
(56) Venuto, P. B. *Adv. Catal.* **1968**, *18*, 259−371.
(57) Venuto, P. B. *Microporous Mater.* **1994**, *2*, 297−411.
(58) Kudo, A.; Kaneko, E. *Chem. Commun.* **1997**, 349−350.
(59) Alvaro, M.; García, H.; García, S.; Marquez, F.; Scaiano, J. C. *J. Phys. Chem.* **1997**, *101*, 3043−3051.
(60) Argauer, R. J.; Landlolt, G. R. U.S. Patent **1982**, 3 702 886.